Available online at www.sciencedirect.com
SCIENCE DIRECT®
Journal of Solid State Chemistry 178 (2005) 2608–2612
JOURNAL OF SOLID STATE CHEMISTRY
www.elsevier.com/locate/jssc

# Metastability of atomic ordering in lead–strontium nitrate solid solutions

A.G. Shtukenberg*

*Crystallography Department, St. Petersburg State University, Universitetskaya emb., 7/9, 199034, St. Petersburg, Russia*

Received 11 March 2005; received in revised form 28 April 2005; accepted 15 May 2005
Available online 11 July 2005

**Abstract**

A decrease in the anomalous birefringence of ostensibly cubic crystals of $(Pb,Sr)(NO_3)_2$ during annealing between 280–450 °C shows first-order reaction kinetics with Arrhenius-like temperature dependence. The activation energies associated with this process were 111(5) and 359(17) kJ/mol below 370 °C and above 400 °C, respectively. Such behavior agrees with theoretical predictions and confirms that the ordering of cations is the primary cause of the anomalous birefringence.


*Keywords:* Kinetic phase transition; Lead nitrate; Strontium nitrate; Desymmetrization; Solid solution; Optical anomalies; Diffusion

## 1. Introduction

Kinetic ordering of atoms, ions, or molecules in crystals, sometimes referred to as "growth ordering" or "growth desymmetrization", is a type of order–disorder phase transformation. This non-equilibrium process can arise when crystallographic sites related by symmetry in the bulk are geometrically and energetically distinct on the surfaces of a growing crystal. Such sites express different activities for adsorbing chemical species, thereby reducing the symmetry of the surface layer that subsequently becomes buried in the bulk. Metastable distributions of crystal components of this kind can persist for very long times due to the low diffusion rates in solids. The differential site occupancies result in distortions of the crystal structure giving physical properties that are excluded by symmetry in the corresponding structure at equilibrium.

Desymmetrization due to kinetic ordering is often apparent in optical measurements. Crystals showing lower optical symmetries than might be expected on the basis of their morphology or X-ray analysis are called *optically anomalous*. Optical anomalies have been discovered and studied in many substances including [1] quartz, alums [2,3], garnets [4,5], topaz [6], $Na(ClO_3, BrO_3)$ [7,8].

One of the main features of kinetic growth ordering is metastability. At high temperatures ($T/T_{melt} > 0.6$) the degree of ordering decreases rapidly with a corresponding decrease of anomalous birefringence. This phenomenon was found to occur in topaz [6], analcite [9], $(Y_{0.53}Nd_{0.47})_3Ga_5O_{12}$ garnets [10] and some other compounds. For the sodium chlorate–bromate isomorphs [7] and grandite garnets [11] the crystal structure refinement carried out before and after high-temperature annealing has shown equalization of occupancies and return to the ideal cubic symmetry. Quantitatively annealing kinetics was studied for quartz [1], alums [2,5] and grandite garnets [5], for which decreasing in birefringence was found to follow the first-order kinetics with a temperature dependence in agreement with the Arrhenius Law.

Anomalous birefringence in the lead–strontium–barium nitrates $(Pb,Sr,Ba)(NO_3)_2$ has been know since the 19th century [12]. While the earliest researchers

*Fax: +7 812 328 4418.
*E-mail address:* sasha@as3607.spb.edu.

0022-4596/$ - see front matter © 2005 Elsevier Inc. All rights reserved.
doi:10.1016/j.jssc.2005.05.009

attributed the anomalous birefringence to strain (Spannung), it was previously suggested that the birefringence was due to growth desymmetrization [13]. Here, we study the temperature dependence of the anomalous birefringence while annealing the mixed crystals. We aim to focus our understanding of the mechanisms of growth desymmetrization and self-diffusion in crystals.

## 2. Experimental

The lead–strontium nitrate $(Pb,Sr)(NO_3)_2$ crystals were grown to sizes of 5–15 mm from unstirred aqueous solutions supercooled by 1–5 °C by self-nucleation in 300–500 mL vessels or by solvent evaporation at the temperature of 29–32 °C. The principal facets expressed were {111}. Smaller {100} were evident. Seldom, very small {210} faces were also observed. Crystal sections (0.6–2 mm) were cut parallel to {110} planes (at the same time normal to {111} growth faces). The values of birefringence $\Delta n$ were measured with a conventional polarizing microscope equipped with a Berek compensator accurate to within 5–10%. According to the data of electron probe microanalysis Sr/Pb distribution within each growth sector is relatively homogeneous (the difference in Sr content does not exceed 0.03 at.fr.). On the other hand, {111} growth sectors are slightly enriched by Sr with respect to {100} ones, the differences in composition increase to the middle of the series and attains 0.06 at.fr. The birefringence was measured at several points within each section before and after annealing in a muffle furnace at a temperature between 280 and 450 °C for times as short as 7 min and as long as 12 h.

### 2.1. Anomalous birefringence and ordering of cations

Lead nitrate $Pb(NO_3)_2$ and strontium nitrate $Sr(NO_3)_2$ belong to the cubic system (space group $Pa\bar{3}$ [14,15] or $P2_13$ [16,17]); they are optically isotropic as required by symmetry. The compounds form a continuous series of solid solutions well known for their anomalous birefringence [12].

The {111} growth sectors are optically uniaxial negative with the optical axis $X_{(\varepsilon)}$ directed normal or nearly normal (deviations with a few degrees) to the respective growth face. The value $\Delta n$ can be as high as $1.6\times10^{-3}$ in the middle of the series, but it decreases towards the end members. Usually the birefringence is distributed uniformly throughout the growth sector; however, thin zones with gradually or even sharply changing birefringence were frequently observed. Assuming that the crystal symmetry after desymmetrization is a subgroup of the cubic group of the pure materials—symmetry is destroyed but not created—then the mixed crystals are presumably trigonal. The similar optical patterns were also observed for the $(Pb,Ba)(NO_3)_2$ solid solutions [13].

In contrast to the {111} growth sectors, the {100} sectors display a much smaller value of $\Delta n$ (typically less than $5\times10^{-5}$) and are inhomogeneous with respect to the distribution of birefringent areas. The optical indicatrix orientation as well as the value of birefringence reveals a complicated or even oscillatory thin zoning, also typical for {100} growth sectors of alum mixed crystals [3]. This birefringence is stable during annealing and is probably related to intrinsic stress. Therefore, only the {111} growth sectors were further analyzed.

Although the experimental data on the $(Pb,Sr)(NO_3)_2$ crystal structures are lacking, some assumptions can be based on the results obtained for the $(Pb,Ba)(NO_3)_2$ isomorphs. Crystal structure refinement of two $(Pb_{0.1}Ba_{0.9})(NO_3)_2$ birefringent samples cut out from {111} growth sectors showed symmetry reduced to either of the trigonal groups $R\bar{3}$ or $R3$ [13]. The single (0,0,0) cation site was found to split into two sites with different Pb/Ba ratios: a general site [1] with fractional atomic coordinates $(x,y,z)$ and multiplicity 3 and a special site [2] with fractional coordinates $(0,0,z)$ and multiplicity 1 [18]. This model, matching the observed uniaxial optical indicatrix, will be extended to $(Pb,Sr)(NO_3)_2$.

### 2.2. Metastability of growth ordering: theory

We presume that diffusion assisted redistribution of Sr and Pb follows the vacancy mechanism [19]. Assume $P$ to be the probability of cation (vacancy) jumps between neighboring sites. The cations form the face-centered lattice and in the cubic crystal structure have the same surrounding by oxygen atoms. Since the desymmetrization usually has a negligible effect on the geometry of the crystal structure, it would be reasonable to suggest that the jump probability $P$ is nearly the same for the cations located at sites [1] and [2]. In the trigonal structure each [1] site is surrounded by four [2] sites and eight [1] sites, whereas each [2] site is surrounded by twelve [1] sites. Keeping in mind the expression for the average atomic fraction of strontium $\bar{x}=(3x^{[1]}+x^{[2]})/4$, we can write two rate equations that describe the equalization of occupancies:

$$\frac{dx^{[1]}}{dt}=\frac{4}{12}Px^{[2]}+\frac{8}{12}Px^{[1]}-Px^{[1]}=\frac{4}{3}P(\bar{x}-x^{[1]}), \quad (1)$$

$$\frac{dx^{[2]}}{dt}=\frac{0}{12}Px^{[2]}+\frac{12}{12}Px^{[1]}-Px^{[2]}=\frac{4}{3}P(\bar{x}-x^{[2]}). \quad (2)$$

Solution of these equations gives an expression for the reaction progress variable:

$$\xi = \frac{x^{[2]} - x^{[1]}}{x_0^{[2]} - x_0^{[1]}} = \exp\left(-\frac{4}{3} Pt\right), \quad (3)$$

where the subscript "0" denotes the initial values of occupancies, and $t$ is the annealing time. The average self-diffusion coefficient of cations can be written as $D = Ph^2$, where the distance between the neighboring sites $h$ is equal to $\sqrt{2}a/2$, and $a \sim 7.8$ Å is the lattice constant. Presuming that the birefringence $\Delta n$ is proportional to the difference in occupancies $x^{[2]}$–$x^{[1]}$, we can rewrite Eq. (3) as follows:

$$\xi = \frac{\Delta n}{\Delta n_0} = \exp\left(-\frac{4}{3}\frac{Dt}{h^2}\right). \quad (4)$$

Usually in ionic crystals (i.e. also in lead–strontium nitrate) at relatively low temperatures concentration of vacancies is much higher than their equilibrium concentration [20]. In this case migration of atoms proceeds in extrinsic region [20], and the diffusion coefficient is

$$D_{ex} = D_{0ex} \exp\left(-\frac{E_m}{RT}\right), \quad (5)$$

where $D_0$ is proportional to the concentration of vacancies $C_v$, $E_m$ is the activation energy for the vacancy migration, $R$ is the gas constant, and $T$ is the absolute temperature. If $C_v$ corresponds to the equilibrium vacancy concentration (high temperatures, intrinsic region [20]), the expression for the diffusion coefficient includes an additional activation barrier $E_f$ responsible for the vacancy formation:

$$D_{in} = D_{0in} \exp\left(-\frac{E_m + E_f}{RT}\right) \quad (6)$$

For a given initial distribution of cations and diffusion mechanism, Eqs. (4)–(6) should describe the decrease in the anomalous birefringence during the course of annealing. They also give the mutual diffusion coefficient $D = D_{Sr}D_{Pb}/(D_{Pb} + \bar{x}[D_{Sr} - D_{Pb}])$ [19], but not the coefficients of the individual ions $D_{Sr}$ and $D_{Pb}$.

### 2.3. Annealing kinetics: results and discussion

Fig. 1 shows the typical annealing curves plotted for three different points taken in two adjacent {111} growth sectors (average composition $(Pb_{0.38}Sr_{0.62})(NO_3)_2$) at 340 °C. The value of $\ln \xi = \ln(\Delta n/\Delta n_0)$ is inversely proportional to the annealing time ($t$), therefore the rate constant does not appear to change with time. Thus, the process obeys first-order reaction kinetics where $\Delta n = \Delta n_0 \exp(-kt)$, an expression with precisely the form of Eq. (4) that yields the value of the diffusion coefficient $D = 3h^2k/4$.

Annealing at different temperatures shows that $\ln k$ is inversely proportional to the reciprocal of the absolute temperature $1/T$; the birefringence decrease is governed by Arrhenius kinetics (Fig. 2) $k = k_0 \exp(-E_a/RT)$, where $k_0$ is a constant. The activation energy $E_a$ for the annealing temperatures below 370 °C varies for different samples from 98–123 kJ/mol (average value 111(5) kJ/mol). At higher temperatures the slope increases sharply corresponding to a considerably higher activation

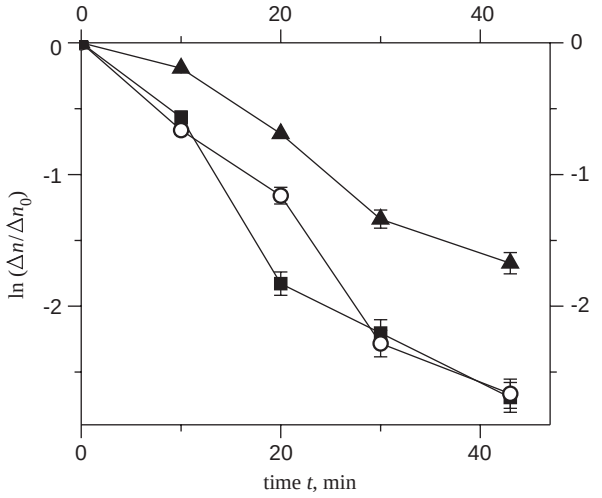


Fig. 1. Decrease in birefringence as a function of annealing time for three different points in two adjacent {111} growth sector (average composition $(Pb_{0.38}Sr_{0.62})(NO_3)_2$) at 340 °C. Error bars if not shown are less than the symbol size.

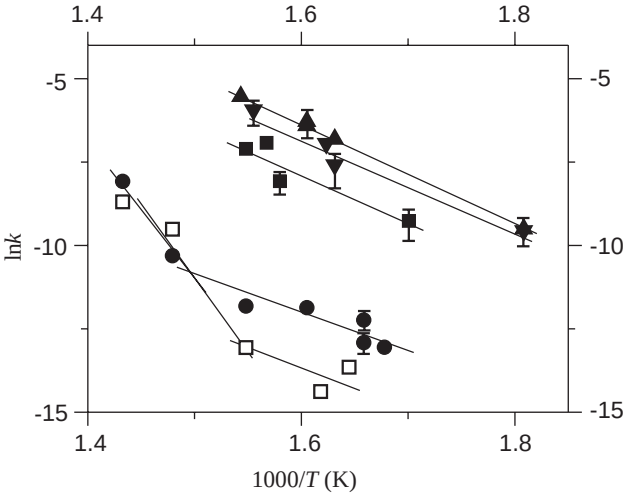


Fig. 2. Arrhenius plot of the rate constant $k$ measured for the transformation from birefringent to isotropic {111} growth sectors from $(Pb,Sr)(NO_3)_2$ solid solutions. Different symbols (squares, circles, up and down triangle) denote different samples; open and filled squares denote different sets of points chosen within one growth sector for the measurement of birefringence. The birefringence is more stable in relative perfect regions of the growth sector (open squares), whereas near to the crystal imperfections (filled squares) it decreases with significantly higher rates. Error bars if not shown are less than the symbol size.

energy (342–376 kJ/mol with the average of 359(17) kJ/mol). It would be reasonable to suggest that the diffusion occurs in the extrinsic region at low temperatures and, according to the Eq. (5), the activation energy necessary for the vacancy migration is $E_a = E_m = 111$ kJ/mol. Lacking data on the diffusion coefficients for the pure nitrates, a direct verification of the suggested mechanism is not possible; however, the $E_a$ is in good agreement with the activation energies for the vacancy motion in various halides (25–105 kJ/mol [20]). On the other hand, diffusion at higher temperatures occurs in the intrinsic regime according to Eq. (6), it should be characterized by the activation energy $E_a = E_f + E_m = 359$ kJ/mol. Thus, the activation energy for the vacancy formation can be estimated as $E_f = 359-111 = 250$ kJ/mol, close to the energies of the various halides 85–250 kJ/mol [20].

The most surprising feature of the annealing behavior is the huge difference in the rate constant $k$ for different points taken in the same growth sector, so that the ratio $k_{max}/k_{min}$ can be as high as $10^3$ (refer to open and filled squares in Fig. 2). Since the activation energies measured for different points are roughly the same, differences must be attributed to the pre-exponential factor $k_0$. Rate constants increase significantly in the vicinity of cracks, liquid inclusions, and sometimes at growth sector boundaries and free surfaces.

Fig. 3 shows the relative change in birefringence during three annealing runs at $T = 275-343\,^{\circ}C$ as a function of distance from a crack, $z$. Such behavior suggests that the fresh crystal surface acts as a source of vacancies that diffuse into the crystal volume and accelerate the self-diffusion and equalization of cation occupancies. In this case, the birefringence should be controlled by the concentrations of vacancies $C_v \propto D_{0ex}$ (see Eqs. (4) and (5)). Since annealing does not affect the homogeneous parts of the crystal, the assumption of negligible vacancy concentration in the beginning of the experiment seems to be reasonable. According to the semi-infinite medium solution to the Fick diffusion Eq. [20,21] the concentration of vacancies $C_v$ decreases with the distance from the crack as

$$C_v = C_{v0}\left(1 - \mathrm{erf}\left[\frac{z}{2\sqrt{D_v t}}\right]\right), \quad (7)$$

where $C_{v0}$ denotes the concentration of vacancies at the free surface and $D_v$ is the diffusion coefficient for the vacancies. An excellent fit of the experimental profile with the function (7) (Fig. 3) confirms the hypothesis suggested and emphasizes the role of vacancies in the reduction of anomalous birefringence.

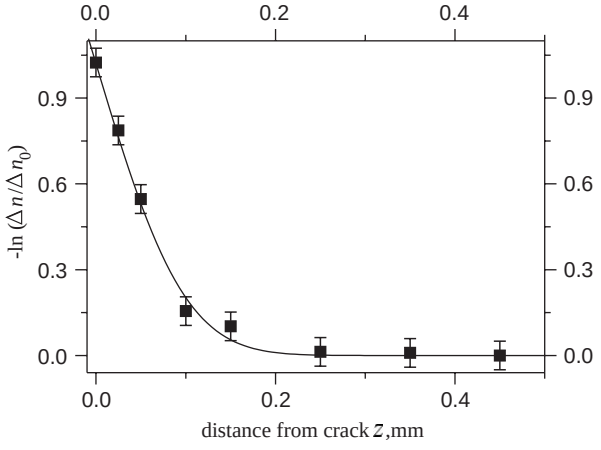


Fig. 3. Changes in birefringence during annealing as a function of the distance from a crack. Points—experiment, line—fit with Eq. (7).

## 3. Conclusion

High-temperature (280–450 °C) annealing of $(Pb,Sr)(NO_3)_2$ solid solutions revealed that the anomalous birefringence in the {111} growth sectors decreases with first-order Arrhenius kinetics. At temperature below 370 °C the activation energy is nearly constant and equal to 111(5) kJ/mol in most regions throughout the prepared plates. This activation energy can be directly associated with the activation energy for the cations (vacancies) migration. Near cracks the rate constant varies over a wide range. At higher temperatures, >400 °C, the activation energy is 359(17) kJ/mol, indicating a distinct dynamic process. This essentially higher value of activation energy corresponds to a sum of activation energies for the cations (vacancies) migration and vacancies formation. The results agree with theoretical predictions and thereby confirm the growth ordering of cations as the principal reason for anomalous birefringence in the $(Pb,Sr)(NO_3)_2$ solid solutions. These conclusion is also in a good agreement with the data provided for the similar $(Pb,Ba)(NO_3)_2$ isomorphous series [13], where the ordering of isomorphous ions was detected with the single crystal X-ray diffraction method.

The comparatively slight birefringence in the {100} growth sectors was stable to annealing and is likely to have another origin, presumably it is due to the intrinsic stress.

## Acknowledgments

This work was supported by the German Academic Exchange Service DAAD (Grant A/04/06089), by INTAS Young Scientist Fellowship program (Grant 2004-83-2826) and by the Russian Foundation for Basic Research RFBR (Grant 05-05-64289). The author also thanks E. Hägele and I.A. Kasatkin for their assistance and B. Kahr for detailed reviewing and improving of the manuscript.

## References


[1] L.I. Tsinober, M.I. Samoilovich, in: B.K. Wainshtein, A.A. Chernov (Eds.), Problems of the Modern Crystallography, Nauka, Moscow, 1975, pp. 207–218 (in Russian).
[2] A.G. Shtukenberg, Yu.O. Punin, O.G. Kovalev, Crystallogr. Rep. 43 (1998) 465–468.
[3] A.G. Shtukenberg, Yu.O. Punin, E. Haegele, H. Klapper, Phys. Chem. Miner. 28 (2001) 665–674.
[4] M. Wildner, M. Andrut, Am. Miner. 86 (2001) 1231–1251.
[5] A.G. Shtukenberg, Yu.O. Punin, Optical Anomalies in Crystals, Nauka, St. Petersburg, 2004 (in Russian).
[6] M. Akizuki, M.C. Hampar, J. Zussman, Miner. Mag. 43 (1979) 237–241.
[7] P. Gopalan, M.L. Peterson, G. Crundwell, B. Kahr, J. Am. Chem. Soc. 115 (1993) 3366–3367.
[8] A.G. Shtukenberg, I.V. Rozhdestvenskaya, D. Yu. Popov, Yu.O. Punin, J. Solid State Chem. 177 (2004) 4732–4742.
[9] Náray-Szabó, Z. Krist. 99 (1938) 291.
[10] K. Kitamura, N. Iyi, S. Kimura, F. Cherrier, J.M. Davignes, H. Le Gall, J. Appl. Phys. 60 (1986) 1486–1489.
[11] F.M. Allen, P.R. Buseck, Am. Miner. 73 (1988) 568–584.
[12] R. Brauns, Die optischen Anomalien der Kristalle, Preisschr. Jablonowski-Ges., Leipzig, 1891.
[13] P. Gopalan, B. Kahr, J. Solid State Chem. 107 (1993) 563–567.
[14] H. Nowotny, G. Heger, Acta. Cryst. C 39 (1983) 952–956.
[15] H. Nowotny, G. Heger, Acta. Cryst. C 42 (1986) 133–135.
[16] L.N. Rashkovich, B. Yu. Shekunov, V.N. Voitsekhovsii, M.V. Shvedova, Sov. Phys. Cryst. 34 (1989) 925–928.
[17] D.K. Arkhipenko, E.N. Fedorova, A.P. Shebanin, B.A. Orekhov, in: D.K. Arkhipenko (Ed.), Radiography and Molecular Spectroscopy of Minerals, Nauka, Novosibirsk, 1985, pp. 40–46 (in Russian).
[18] T. Hahn, International Tables for Crystallography, vol. A, Kluwer, Dordrecht, Boston, London, 1993.
[19] J.R. Manning, Diffusion Kinetics for Atoms in Crystals, D. Van Nostrand Company Inc., Princeton, Toronto, 1968.
[20] A. Lasaga, Rev. Miner. 8 (1981) 261–320.
[21] J. Crank, The Mathematics of Diffusion, Oxford University Press, Oxford, 1975.